Positron-annihilation momentum density in superconductors

R. Benedek
Materials Science Division, Argonne National Laboratory, Argonne, Illinois 60439

H.-B. Schüttler
*Center for Simulational Physics, Department of Physics and Astronomy, University of Georgia, Athens, Georgia 30602**
and Materials Science Division, Argonne National Laboratory, Argonne, Illinois 60439

(Received 18 August 1989)

The origin of the dramatic shifts observed in the temperature dependence of positron-annihilation characteristics (particularly lifetime and Doppler-broadening line shape) near T_c in the cuprates is not presently clear. Both intrinsic and extrinsic (i.e., defect-related) mechanisms have been proposed. To help clarify whether Cooper pairing is responsible for these shifts, we present an approximate formulation of the positron characteristics in a BCS superconductor. Relations are derived for the zeroth- and first-order terms in the ladder summation for the two-photon momentum density, with electron propagators represented in the Nambu-Gorkov form. The momentum densities in the normal and superconducting states differ appreciably only within the pairing shell centered at p_F. Numerical calculations are performed for two- and three-dimensional models. The differences increase with increasing Δ/μ but are relatively small in the first-order calculation. We also estimate an upper bound to the effect of BCS pairing on the positron characteristics, including terms to all orders in the electron-positron interaction. Based on comparisons of our model calculations with experiment, it seems unlikely that BCS pairing is responsible for the measured shifts in positron properties near T_c.

I. INTRODUCTION

Positron-annihilation spectroscopy (PAS) is sensitive to the electronic charge and momentum densities in materials.[1] Since both types of density distributions vary with the phase of a given material, PAS can, in principle, serve as a probe of solid-state phase transitions. Although structural phase transitions and charge-density waves (CDW's) have been studied extensively[1] with PAS, the onset of superconductivity[2] (at least in conventional materials[2,3]) has shown no measurable effect. This insensitivity is actually not surprising, since the positron interacts with the entire electron sea, which is only slightly perturbed by superconductivity in systems where the gap parameter Δ is orders of magnitude smaller that the Fermi energy μ. Measurements on the cuprate superconductors,[3-8] however, have shown significant shifts near T_c. These new results raise the question of whether superconductive pairing in high-T_c materials, which have relatively large values of Δ/μ, would give rise to measurable changes in positron-annihilation characteristics. At the present time, the experimental picture requires further clarification,[9] and the possible role of thermal detrapping as a source of lifetime temperature dependence cannot be discounted.[10,11] The lifetime observations of Refs. 3-5, however, have attracted considerable attention, since they appear to manifest a direct probe of the bulk superconductivity.[12]

Jean *et al.*[3,5] (and Harshman *et al.*[4]) report positron lifetimes in the superconducting state that increase linearly with decreasing temperature for $Tl_2Ba_2CaCu_2O_8$ and $YBa_2Cu_3O_{6,9}$ and are 5-15 % larger at 0 K than the extrapolated normal-state values. If we assume that this behavior is intrinsic, i.e, related to annihilation from a delocalized positron state, there are still a number of mechanisms that may be responsible: (i) a shift in the electronic charge density $n(r)$ in the superconductor,[12] (ii) a structural phase transition or a shift in the phonon spectrum, and (iii) a shift in electron-positron correlations because of superconductive pairing. Although (i) and (ii) cannot be entirely dismissed at this time, the third possibility has generated the most interest, since positron measurements might then enable discrimination between alternative models of superconductivity. The remainder of this paper will focus on the effect of electron-positron correlations on positron characteristics.

Little detailed theory exists regarding PAS in superconductors. In recent work, the lifetime of extended positron states in CuO_2 planes has been studied by Chakraborty employing a real-space pairing model,[13] and by McMullen based on the (paired-boson) resonating-valence-bond (RVB) picture.[14] The only theory of PAS in superconductors preceding high T_c was that of Tripathy and Bhuyan,[15] who derived a first-order perturbation treatment of the lifetime based on the BCS theory but performed only a limited numerical analysis.

In this paper we present a first-order treatment of the two-photon momentum density in a BCS superconductor.[16] Before any judgment is made regarding exotic mechanisms,[13,14] it is important to explore first the consequences of the conventional model. The momentum density enables predictions of the lifetime as well as angular correlation and Doppler broadening. Although the life-

time has manifested the most dramatic temperature dependences, it seems unwise to focus entirely on this property, which in itself conveys very limited information. It is well known that a first-order treatment considerably underestimates absolute enhancement factors.[17] however we will see that it does provide considerable insight and, in particular, suggests a way to estimate an upper bound on the effect of BCS pairing on the positron characteristics.

II. FORMULATION OF TWO-PHOTON MOMENTUM DENSITY

We investigate the effect of superconductivity on the partial-annihilation rate, or two-photon momentum density. Projections of the two-photon momentum density are measured in angular correlation or Doppler-broadening experiments,[18] and the positron lifetime is inversely proportional to the integral of the momentum density over all momenta. As mentioned earlier, we treat superconductivity within the BCS framework.

The two-photon momentum density can be expressed[19] in terms of the imaginary-time correlation function (atomic units are used throughout)

$$R(\tau,\mathbf{p})\equiv\lambda/\Omega\int d^3x\, d^3y e^{-i\mathbf{p}\cdot(\mathbf{x}-\mathbf{y})}R(\tau,\mathbf{x},\mathbf{y}) , \quad (2.1)$$

where λ is a constant, Ω is the specimen volume, and

$$R(\tau,\mathbf{x},\mathbf{y})\equiv\langle T_\tau A^\dagger(\mathbf{x},\tau)A(\mathbf{y},0)\rangle . \quad (2.2)$$

Here $A(\mathbf{x})\equiv\psi_\uparrow(\mathbf{x})\,\phi_\downarrow(\mathbf{x})$ destroys an electron-positron pair (with opposite spins), $O(\tau)\equiv e^{\tau H}O(0)e^{-\tau H}$, for imaginary-time Heisenberg operator O, and the angular brackets in Eq. (2.2) denote a (two-component plasma) grand-canonical-ensemble average.[20]

The (unnormalized) two-photon momentum density can be expressed as

$$R(\mathbf{p})=R(\tau=0^-,\mathbf{p}) . \quad (2.3)$$

Since $R(\mathbf{p})$ is proportional to the number of positrons N_p, we apply a normalization factor

$$N_p\equiv\int d^3x\langle\phi_\downarrow^\dagger(\mathbf{x})\phi_\downarrow(\mathbf{x})\rangle = \sum_{\mathbf{k}}\langle\phi_{\mathbf{k}\downarrow}^\dagger\phi_{\mathbf{k}\downarrow}\rangle=\sum_{\mathbf{k}}n_F(\eta_{\mathbf{k}}) , \quad (2.4)$$

where

$$\phi_\downarrow(\mathbf{x})\equiv\Omega^{-1/2}\sum_{\mathbf{k}}e^{i\mathbf{k}\cdot\mathbf{x}}\phi_{k\downarrow} ,$$

$$n_F(x)\equiv(e^{\beta x}+1)^{-1}$$

is the Fermi function, and $\eta_{\mathbf{k}}\equiv\zeta_{\mathbf{k}}-\mu_p$ is the positron energy ($\zeta_{\mathbf{k}}\equiv k^2/2m_p$) relative to its chemical potential μ_p; m_p is the effective mass of the positron. [In Eq. (2.4) we have for convenience taken the positron to be spin down; the results for a spin-up positron would, of course, be the same in paramagnetic medium.] Thus, the normalized two-photon momentum density is given by

$$r(\mathbf{p})\equiv r(\tau=0,\mathbf{p})\equiv R(\tau=0,\mathbf{p})/N_p , \quad (2.5)$$

where $R(\tau=0,\mathbf{p})$ and N_p are taken in the dilute limit, i.e., $\mu_p\to-\infty$. In this limit, both $R(\tau=0,\mathbf{p})$ and N_p are proportional to $\exp(\mu_p/T)$.

III. ZEROTH- AND FIRST-ORDER TERMS

We evaluate the zeroth- and first-order terms (Feynman diagrams) in the ladder expansion for $R(\tau,\mathbf{p})$, treating the normal and the superconducting states to the same level of approximation. The significance of higher-order terms will be considered in Sec. VI. Relations for the Nambu Green's functions[21] employed in the derivations are collected in Appendix A.

A. Zeroth order

The zeroth-order term can be expressed as

$$R^0(\tau,\mathbf{p})=\lambda\Omega^{-1}\sum_{\mathbf{k}}G_e(\tau,\mathbf{k})G_p(\tau,\mathbf{p}-\mathbf{k}) , \quad (3.1)$$

where $G_e(\tau,\mathbf{k})$ is the projected spin-up component of the electron Green's function, i.e.,

$$G_e(\tau,\mathbf{k})\equiv\hat{t}_\uparrow^\dagger\hat{G}_e(\tau,\mathbf{k})\hat{t}_\uparrow ,$$

where $\hat{t}_\uparrow$ is the spinor

$$\begin{bmatrix}1\\0\end{bmatrix} ,$$

and $\hat{G}_e$ is the 2×2 Nambu Green's-function matrix.[21] We obtain

$$R^0(\mathbf{p})=R^0(\tau=0^-,\mathbf{p})=\lambda(2\pi)^{-3}\int d^3k[u_{\mathbf{k}}^2n_F(E_{\mathbf{k}})+v_{\mathbf{k}}^2n_F(-E_{\mathbf{k}})]n_F(\eta_{\mathbf{p}-\mathbf{k}}) . \quad (3.2)$$

The positron density, Eq. (2.4), is given by

$$N_p=(2\pi)^{-3}\int d^3k\, n_F(\eta_{\mathbf{k}})=(m_pT/2\pi)^{3/2}\exp(\beta\mu_p),\quad \mu_p\to-\infty , \quad (3.3)$$

and the normalized momentum density, according to Eq. (2.5), is then

$$r^0(\mathbf{p})\equiv R(\tau=0,\mathbf{p})/N_p=\lambda\Omega^{-1}(2\pi m_pT)^{-3/2}\int d^3k[u_{\mathbf{k}}^2n_F(E_{\mathbf{k}})+v_{\mathbf{k}}^2n_F(-E_{\mathbf{k}})]\exp(-\beta\zeta_{\mathbf{p}-\mathbf{k}}) . \quad (3.4)$$

A number of limiting cases can be obtained directly from Eq. (3.4). For example, in the zero-temperature, zero-gap limit, we have

$$r^0(\mathbf{p})=\Theta(-\xi_{\mathbf{p}})\ (\Delta=0,\quad T=0) , \quad (3.5)$$

where Θ is the unit-step function, and $\xi_{\mathbf{p}}\equiv p^2/2m_e-\mu_e$; the normalization factor $\lambda\Omega^{-1}$ is omitted. In the zero-

temperature limit we have the electron-momentum distribution for a BCS superconductor

$$r^0(\mathbf{p})=v_{\mathbf{p}}^2, \quad (T=0) . \tag{3.6}$$

The zero-gap limit ($\Delta=0$) at finite temperature is given by

$$r^0(\mathbf{p})=(2\pi m_p T)^{-3/2}\int d^3k\, n_F(\xi_{\mathbf{k}})\exp(-\beta\zeta_{\mathbf{p}-\mathbf{k}}) \quad (\Delta=0) . \tag{3.7}$$

A low-temperature expansion of $r^0(\mathbf{p})$ is presented in Appendix B.

B. First-order term

Assuming a static electron-positron interaction $V(q)$, discussed in Sec. IV, the first-order contribution to $R(\tau,\mathbf{p})$ can be expressed (in the spectral representation) as

$$R^1(\tau,\mathbf{p})=\lambda T^3\Omega^{-1}\sum_{i\omega} e^{-i\omega\tau}\sum_{\mathbf{k}_1\mathbf{k}_2}\sum_{i\nu_1 i\nu_2}\hat{t}_\uparrow^\dagger\hat{G}_e(i\nu_2,\mathbf{k}_2)\hat{\tau}_3\hat{G}_e(i\nu_1,\mathbf{k}_1)\hat{t}_\uparrow V(|\mathbf{k}_2-\mathbf{k}_1|)G_p(i(\omega-\nu_2),\mathbf{p}-\mathbf{k}_2)G_p(i(\omega-\nu_1),\mathbf{p}-\mathbf{k}_1) , \tag{3.8}$$

where $i\omega\equiv 2n\pi T$, $i\nu_{1,2}\equiv(2n+1)\pi T$, and τ_3 is the Pauli matrix

$$\begin{bmatrix}1 & 0\\ 0 & -1\end{bmatrix} .$$

After extensive manipulation, we obtain

$$\begin{aligned} r^1(\mathbf{p})=r^1(\tau=0^-,\mathbf{p})=&-\lambda(2\pi)^{-6}\int d^3k_1\, d^3k_2 \\ &\times\{[u^2(\mathbf{k}_2)u^2(\mathbf{k}_1)+u(\mathbf{k}_1)u(\mathbf{k}_2)v(\mathbf{k}_1)v(\mathbf{k}_2)]D_{++}(\mathbf{p},\mathbf{k}_1,\mathbf{k}_2) \\ &+[v^2(\mathbf{k}_2)v^2(\mathbf{k}_1)+u(\mathbf{k}_1)u(\mathbf{k}_2)v(\mathbf{k}_1)v(\mathbf{k}_2)]D_{--}(\mathbf{p},\mathbf{k}_1,\mathbf{k}_2) \\ &+[u^2(\mathbf{k}_1)v^2(\mathbf{k}_2)-u(\mathbf{k}_1)u(\mathbf{k}_2)v(\mathbf{k}_1)v(\mathbf{k}_2)]D_{+-}(\mathbf{p},\mathbf{k}_1\mathbf{k}_2) \\ &+[u^2(\mathbf{k}_2)v^2(\mathbf{k}_1)-u(\mathbf{k}_1)u(\mathbf{k}_2)v(\mathbf{k}_1)v(\mathbf{k}_2)]D_{-+}(\mathbf{p},\mathbf{k}_1,\mathbf{k}_2)\} \\ &\times 2V(|\mathbf{k}_2-\mathbf{k}_1|)(2\pi/m_pT)^{3/2}\exp(\beta\zeta_{\mathbf{p}-\mathbf{k}1}) , \end{aligned} \tag{3.9}$$

where

$$D_{\sigma_1\sigma_2}(\mathbf{p},\mathbf{k}_1,\mathbf{k}_2)\equiv\frac{n_F(-\sigma_2E_{\mathbf{k}_2})n_F(\sigma_1E_{\mathbf{k}_1})}{(\sigma_2E_{\mathbf{k}_2}+\zeta_{\mathbf{p}-\mathbf{k}_2})-(\sigma_1E_{\mathbf{k}_1}+\zeta_{\mathbf{p}-\mathbf{k}_1})} . \tag{3.10}$$

The numerator of $D_{\sigma_1\sigma_2}$ represents the phase space available for an electron to scatter from initial state $\mathbf{k}_1$ to final state $\mathbf{k}_2$ (while the positron scatters from $\mathbf{p}-\mathbf{k}_1$ to $\mathbf{p}-\mathbf{k}_2$) and the denominator represents the energy difference for the process. The $(-,+)$ sign of σ corresponds to states (inside, outside) the ($T=0$) electron Fermi surface.

In the limit $T\to 0$, only the term involving D_{-+} survives. When a dynamical interaction $V(q,\omega)$ is considered, the D_{-+} term gives rise to a weak tail in $r^1(\mathbf{p})$ that extends beyond the Fermi edge ($p>p_F$),[17] which is not relevant to the present discussion. The validity of the static-interaction approximation is discussed by Carbotte and Kahana.[17] The zero-temperature limit of Eq. (3.9) is

$$r^1(\mathbf{p})=-\lambda\Omega^{-1}\int\frac{d^3k}{(2\pi)^3}\frac{u_{\mathbf{k}}^2v_{\mathbf{p}}^2-u_{\mathbf{p}}v_{\mathbf{p}}u_{\mathbf{k}}v_{\mathbf{k}}}{\zeta_{\mathbf{p}-\mathbf{k}}+E_{\mathbf{k}}+E_{\mathbf{p}}} \times 2V(|\mathbf{k}-\mathbf{p}|) \quad (T=0) . \tag{3.11}$$

The combination of coherence factors in the numerator of Eq. (3.11) also occurs, for example, in the formulation of the optical conductivity.[22] The energy denominator in Eq. (3.11) is reminiscent of the random-phase approximation (RPA) susceptibility, but with a singularity at p_F rather than at (the spanning wave vector) $2p_F$. Numerical calculations based on Eq. (3.11) will be presented later.

For the normal state, Eq. (3.11) reduces to

$$r^1(\mathbf{p})=-\lambda\Omega^{-1}\int\frac{d^3k}{(2\pi)^3}\frac{\Theta(\xi_{\mathbf{k}})\Theta(-\xi_{\mathbf{p}})}{\zeta_{\mathbf{p}-\mathbf{k}}+\xi_{\mathbf{k}}-\xi_{\mathbf{p}}} \times 2V(|\mathbf{k}-\mathbf{p}|) \quad (\Delta=0,\ T=0) , \tag{3.12}$$

which is identical to Eq. (2.3) of Carbotte and Kahana.[17]

IV. ELECTRON-POSITRON INTERACTION

The electron-positron interaction will be represented in numerical calculations of $r^1(\mathbf{p})$ by Thomas-Fermi potentials appropriate to two- and three-dimensional systems. In the three-dimensional (3D) case, we have

$$V(q)=-4\pi/(q^2+q_s^2) \quad (3\mathrm{D}) , \tag{4.1}$$

where q_s is the screening wave vector. q_s^2 is related to the irreducible polarization part, whose form for a BCS superconductor was derived by Prange.[23] McMullen[14] has

recently obtained the relation

$$(q_s^2)_s=(q_s^2)_n[1+f(\Delta/\mu)] , \quad (4.2)$$

for small Δ/μ where $(q_s^2)_n=4k_F/\pi$ corresponds to the normal state, and

$$f(x)\sim(x^2/8)(\ln x-0.332) . \quad (4.3)$$

For realistic values of x (see the following), however, the correction term f is negligible.

A two-dimensional (2D) analog to Eq. (4.1) was derived by Stern,[24] based on an evaluation of the Lindhard polarizability for a planar system:

$$V(q)=-2\pi/[q+2g(q)] \quad (2D) , \quad (4.4)$$

where

$$g(q)=1-[1-(2k_F/q)^2]^{1/2}\Theta(q-2k_F) .$$

The screening is independent of electron density[25] in this treatment. Since the Stern model is derived for a slab geometry, one may question its applicability to the cuprates, which have three-dimensional character. Nevertheless, it does model in some fashion the strongly anisotropic character of such systems, and has the advantage of analytical tractability.

Although more precise forms than Eqs. (4.1) and (4.4), i.e., including electron-electron correlations, are available, the trends in the numerical results described later are relatively insensitive to the potential. Some analytical results for $r^1(\mathbf{p})$ based on Eqs. (4.1) and (4.4) are presented in Appendix C.

V. NUMERICAL CALCULATIONS

As noted previously, the dominant contributions to $r^1(p)$ in Eq. (3.9) is the term involving D_{-+}, the zero-temperature limit of which is given by Eq. (3.11). Numerical evaluations were performed for two-dimensional as well as three-dimensional models (2D and 3D). [In the two-dimensional model $d^3k/(2\pi)^3$ is replaced by $d^2k/(2\pi)^2$ in Eq. (3.13).]

The calculations require specification of five input parameters: the electron Fermi energy μ, the gap parameter Δ, the pairing-shell width ω_0 [cf. Eq. (A6)], and the effective electron and positron masses m_e and m_p. Calculations were performed for the three sets of parameters described in Sec. V A.

Measured positron-annihilation characteristics can be expressed in terms of moments

$$M_j=\int r(p)p^j dp$$

of the momentum density (apart from instrumental resolution, which we neglect). For example, the lifetime τ for a three-dimensional system is proportional to the reciprocal of M_2 and the Doppler-broadening line-shape parameter S is proportional to M_1/M_2. Since the effect of superconductivity is to shift the first few moments in the same sense (i.e., negatively, as shown in Table I), the relative change in τ is expected to be greater than that in S in going from the normal to the superconducting state.

TABLE I. Numerical results for zeroth, first, and second moments of the two-photon momentum density for superconducting (s) and normal (n) states, in three-dimensional (3D) and two-dimensional (2D) models. Parameters for models (A,B,C): $\mu=(1.5,0.3,0.3)$ eV, $m_e=(1,5,1)$, $m_p=1$, $\Delta=30$ meV, $\omega_0=100$ meV.

Model	M_0	M_1	M_2
A, 3D, *n*	1.0740×10^{0}	1.8064×10^{-1}	4.0302×10^{-2}
A, 3D, *s*	1.0731	1.8039	4.0230
A, 2D, *n*	1.0151	1.7183	3.8516
A, 2D, *s*	1.0144	1.7166	3.8470
B, 3D, *n*	0.9950	1.6593	3.6817
B, 3D, *s*	0.9913	1.6436	3.6835
B, 2D, *n*	1.5019	2.5787	5.8330
B, 2D, *s*	1.4847	2.5315	5.7113
C, 3D, *n*	0.7021	0.5263	0.5239
C, 3D, *s*	0.6976	0.5221	0.5209
C, 2D, *n*	0.5619	0.4239	0.4240
C, 2D, *s*	0.5568	0.4184	0.4184

A. Model parameters

Calculations were performed for three models (A,B,C) designed to roughly mimic the cuprates and also to illustrate the effect of bandwidth narrowing, due either to effective-mass renormalization or to a reduced effective number of carriers. The same sets of parameters were used for both the 2D and 3D cases. Model A is based on the parameter set $\mu=1.5$ eV, $p_F=0.332$ a.u., $\Delta=30$ meV, $\omega_0=100$ meV, and $m_e=m_p=1$. The number of electrons enclosed in a Fermi circle with the p_F value just given corresponds to that in a half-filled CuO_2 square-plane band with lattice parameter $a=4.0$ Å. The chosen gap parameter Δ is comparable to the largest values extracted from either tunneling or infrared reflectivity measurements on $YBa_2Cu_3O_{6.9}$.[26] In general, ω_0 is expected to be somewhat larger than Δ. The selected value of $\omega_0=100$ meV, which is consistent with the hierarchy $\mu\gg\omega_0\gg\Delta$, is at the upper limit of the range compatible with a (conventional BCS-Eliashberg) phonon mechanism, and at the lower end of that compatible with an electronic-pairing mechanism. The assumption of a larger value of ω_0, however, would not affect any of our conclusions. Local-density-approximation electronic-structure calculations[3,27,28] have shown an in-plane positron band mass close to the free-fermion value, and m_p was therefore taken to be unity.

In model B, an electron effective mass $m_e=5$ is employed, with the Fermi energy $\mu'=\mu/m_e=0.3$ eV reduced correspondingly. The electron density, pairing-shell thickness ω_0, gap parameter, and Fermi wave vector are the same as in model A. This model roughly represents a tight-binding valence band, in contrast to the free-electron-like band of model A. Since no correction is made for the fact that the electronic spectrum becomes free electron like at sufficiently high energies [e.g., as E_k becomes large in Eq. (3.13)], model B somewhat overestimates the effect of electron-mass renormalization.

In model C, we use the same Fermi energy, $\mu=0.3$ eV, as in model B, but with $m_e=1.0$. This choice corre-

sponds to a smaller density of carriers, specifically a 10% filled band. The other parameters are the same as in models *A* and *B*.

The models just described refer only to the valence electrons. In the case of $YBa_2Cu_3O_{6.9}$, for example, there are 34 bands in the Cu(*d*)O(*p*) manifold, of which two CuO_2 plane bands and two chain bands cross the Fermi level. Therefore, at the independent-particle model level,[27] even neglecting the low positron affinity for the planes,[8,28] the background signal resulting from filled bands is about an order of magnitude larger than that of the valence bands. Since the mean enhancement factor (per electron) for the valence band is probably less than a factor of 2 greater than that of the filled bands,[29] the sensitivity of positron characteristics to the valence electrons is expected to be reduced by close to an order of magnitude because of the filled-band background.

B. Results

1. Zero temperature

The momentum densities $r(p)=r^0(p)+r^1(p)$ for the 2D and 3D versions of model *B* are shown in Fig. 1. Qualitatively similar behavior is observed for the other two models (*A* and *C*). The curve for the normal state shows the Fermi-edge discontinuity, whereas the curve for the superconducting state is smeared over the pairing region bounded by

$$p_{\pm}=[2m_e(\mu\pm\omega_0)]^{1/2}\approx(1\pm0.2)p_F \ .$$

Incidentally, a small discontinuity occurs in the momentum density for a superconductor at momenta $p_{\pm}$ because of the discontinuity of the gap parameter [cf. Eq. (A6)].

We note that the momentum density for the normal state is relatively flat near the Fermi edge in the 3D system in contrast to the slight peaking tendency observed in the 2D case. This behavior reflects the singularity at the Fermi edge associated with the energy denominator in Eq. (3.12).

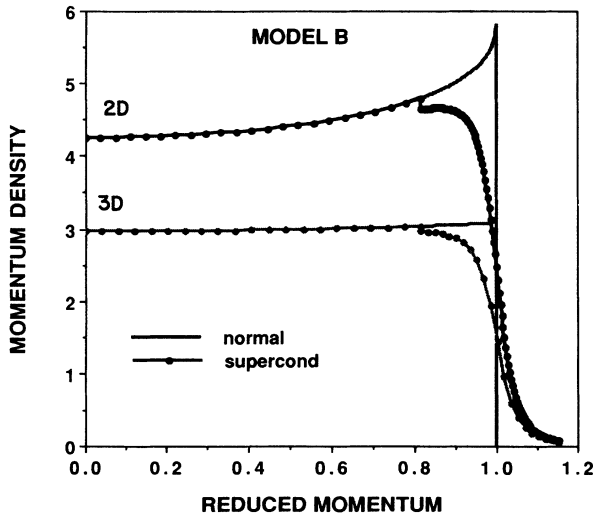

FIG. 1. Momentum density $r(p)=r^0(p)+r^1(p)$ vs reduced momentum p/p_F calculated for model *B* (cf. Table I). The curves with discontinuities at $p/p_F=1$ correspond to the normal state and the dotted curves represent the superconductor. The small discontinuities that occur in the superconducting case at $p_-=0.815$ and $p_+=1.16$ result from the abrupt cutoff of the gap function at ω_0, as given in Eq. (A6). A momentum density of unity would correspond to a noninteracting system.

The zeroth through the second moments of $r(p)$ for models *A*, *B*, and *C* are given in Table I. The results for the normal and superconducting states are very similar (differences less than 1%) for all the 3D models. The largest changes from the normal to the superconducting state occur in the case of the 2D versions of models *B* and *C*. In model *B*, for example, the lifetime (proportional to $1/M_1$) is 1.8% longer in the superconducting than the normal state.

2. Temperature dependence

Temperature dependence in Eq. (3.9) arises from the gap parameter, the positron Boltzmann factor, and the electron Fermi factor. To establish the general trend, we consider only the temperature dependence of the gap parameter, in which case Eq. (3.9) reduces to Eq. (3.11). The lifetime was found to have a temperature dependence similar to the gap parameter itself;[30] it increases with decreasing temperature and is nearly saturated at a reduced temperature of 0.5.

VI. EFFECT OF HIGHER-ORDER CONTRIBUTIONS

The effect of superconductivity on positron-annihilation characteristics was found in the aforementioned calculations to be greatest in the 2D narrow-band models (*B* and *C*). The differences between the moments M_j for normal and superconducting states in 2D models *B* and *C* can largely be attributed to the pronounced (normal-state) edge enhancement between p_- and p_F, which essentially disappears in the superconductor.[31] In fact, a reasonable upper-bound estimate of the relative change

$$\Delta M_0/(M_0)_n\equiv[(M_0)_n-(M_0)_s]/(M_0)_n$$

is given by

$$\int\Delta r(p)dp\,/\int r(p)dp \ ,$$

where

$$\Delta r(p)=r_n(p)-r_{\rm ref}(p) \ ,$$

with $r_{\rm ref}(p)\equiv r_n(p)$ for $p<p_-$ and $r_{\rm ref}(p)\equiv r_n(p_-)$ for $p_F>p>p_-$. $\Delta M_0/(M_0)_n$ therefore depends sensitively on the edge enhancement in the normal state, and an accurate calculation requires going beyond the first-order treatment considered in the preceding sections.

The problem of a positron in (normal) jellium has been studied extensively over the past three decades, using techniques that in effect sum terms to infinite order. The most prominent of these are based on the Bethe-Goldstone (BG) equation,[17,32,33] the Lippmann-Schwinger equation,[34] or the Sawada-boson formalism.[35] No attempt has yet been made to adapt these methods to a superconductor, although it would be possible in principle to do so. The treatment presented earlier in this pa-

per represents a first-order approximation to the Bethe-Goldstone equation. A somewhat larger relative edge enhancement is predicted by the Bethe-Goldstone equation than by the other methods, and we therefore use results from the BG equation[33] to obtain an upper-bound estimate on $\Delta M_0/(M_0)_n$. Based on Fig. 2 of Ref. 33, which corresponds to $r_s=4$, we find

$$\int \Delta r(p)dp / \int r(p)dp \approx 4\% \text{ for } p_- = 0.8p_F$$

(which is roughly the value of p_- corresponding to models B and C; the conclusion would not be affected by choosing smaller values of p_-). When the background effect due to filled bands is included, as discussed in the preceding section, the upper limit on $\Delta M_0/(M_0)_n$ would be reduced to less than 1%, which is much smaller than the experimental results for lifetime in the cuprates Refs. 3–5 (see the following).

The preceding analysis corresponds to a 3D system; to our knowledge no solutions to the BG equations in two dimensions have been obtained. Our experience with the first-order calculations indicates that the edge enhancement should be more pronounced in two dimensions than in three. Nevertheless, we would expect $\Delta M_0/(M_0)_n$ to be increased by less than an order of magnitude in going from a 3D to a 2D system.

VII. COMPARISON WITH EXPERIMENT

Let us consider how these predictions compare with experimental observations on the cuprates.[3–5]

A. Shift in lifetime

The positron lifetime was observed to be constant at tempertures above T_c, but increased by $\sim 7\%$ on cooling either (Refs. 3–5) $YBa_2Cu_3O_{6.9}$ or (Refs. 3 and 5) $La_{1.85}Sr_{0.15}CuO_4$ from T_c to helium temperature and (Refs. 3 and 5) 15% for $Tl_2Ba_2CaCu_2O_8$. The theoretical upper-bound estimates of $\Delta M_0/(M_0)_n$ described in Sec. V are based on a number of assumptions that are difficult to check. As mentioned, no information is available concerning 2D solutions to the BG equation, which may show a large edge enhancement, particularly for a heavy electron mass. On the other hand, the BG equation probably overestimates the edge enhancement, judging by comparison with more refined calculations.[34,35] Overall, a lifetime shift of 7–15 % would seem to be difficult, although perhaps not impossible to achieve, within the BCS framework.

B. Temperature dependence of lifetime

The experiments[3–5] show a linear temperature dependence for $Tl_2Ba_2CaCu_2O_8$ and $YBa_2Cu_3O_{6.9}$, although a saturating behavior was found for $La_{1.85}Sr_{0.15}CuO_4$. The BCS model predicts saturating behavior, basically because the gap parameter saturates. Therefore, it is difficult to reconcile the measurements of temperature dependence for the first two of these compounds with the BCS model.

C. Doppler-broadening line-shape parameter

The experiments by Jean *et al.*[5] show lifetime and line-shape parameter shifts of the same sign (i.e., positive) in going from the normal to the superconducting state. (We note that other workers[36] have observed negative line-shape-parameter shifts in the superconducting state.) Theory, on the other hand, predicts a positive change in lifetime but a negative change in line-shape parameter.

D. Conclusion

Although there are many uncertainties in the comparisons described earlier the overall impression is that a BCS-like framework is difficult to reconcile with the experimental observations in Refs. 3–5.

ACKNOWLEDGMENTS

This work was supported at Argonne National Laboratory (ANL) by the U.S. Department of Energy, Office of Basic Energy Sciences (BES–Materials Sciences), under Contract No. W-31-109-ENG-38. H.-B.S. received support from the Advanced Computational Methods Center and from the Office of the Vice President for Research at the University of Georgia. This material is based on work supported by the National Science Foundation under Grant No. DMR-8913878. Computational work was performed at the National Magnetic Fusion Energy Computing Center at Lawrence Livermore National Laboratory. We are grateful to T. McMullen for discussions and for making unpublished results available to us. We also acknowledge helpful comments by P. Vashista.

APPENDIX A: ANOMALOUS PROPAGATORS

The Nambu prescription for the electron Green's function in the BCS state has the (2×2) spinor form

$$\hat{G}_e(\tau,\mathbf{k}) \equiv -\langle T_\tau \hat{\psi}_{\mathbf{k}}(\tau)\hat{\psi}^\dagger_{\mathbf{k}}(0)\rangle \ , \tag{A1}$$

where the diagonal (11,22) elements are

$$G_e(\tau,\mathbf{k}) \equiv \langle T_\tau \psi_{\mathbf{k}\uparrow}(\tau)\psi^\dagger_{\mathbf{k}\uparrow}(0)\rangle \ ,$$

$$\bar{G}_e(\tau,\mathbf{k}) \equiv \langle T_\tau \psi^\dagger_{-\mathbf{k}\downarrow}(\tau)\psi_{-\mathbf{k}\downarrow}(0)\rangle \ ,$$

and off-diagonal (12,21) elements are

$$F_e(\tau,\mathbf{k}) \equiv \langle T_\tau \psi_{\mathbf{k}\uparrow}(\tau)\psi_{-\mathbf{k}\downarrow}(0)\rangle \ ,$$

$$\bar{F}_e(\tau,\mathbf{k}) \equiv \langle T_\tau \psi^\dagger_{-\mathbf{k}\downarrow}(\tau)\psi^\dagger_{\mathbf{k}\uparrow}(0)\rangle \ .$$

In the spectral representation, one has

$$G_e(i\nu,\mathbf{k}) = \frac{u_{\mathbf{k}}^2}{i\nu - E_{\mathbf{k}}} + \frac{v_{\mathbf{k}}^2}{i\nu + E_{\mathbf{k}}} \ ,$$

$$\bar{G}_e(i\nu,\mathbf{k}) = \frac{v_{\mathbf{k}}^2}{i\nu - E_{\mathbf{k}}} + \frac{u_{\mathbf{k}}^2}{i\nu + E_{\mathbf{k}}} \ ,$$

$$F_e(i\nu,\mathbf{k}) = \frac{\alpha_{\mathbf{k}} u_{\mathbf{k}} v_{\mathbf{k}}}{i\nu - E_{\mathbf{k}}} - \frac{\alpha_{\mathbf{k}} u_{\mathbf{k}} v_{\mathbf{k}}}{i\nu + E_{\mathbf{k}}} \ ,$$

$$\bar{F}_e(i\nu,\mathbf{k}) = \frac{\alpha^*_{\mathbf{k}} u_{\mathbf{k}} v_{\mathbf{k}}}{i\nu - E_{\mathbf{k}}} - \frac{\alpha^*_{\mathbf{k}} u_{\mathbf{k}} v_{\mathbf{k}}}{i\nu + E_{\mathbf{k}}} \ ,$$

where

$$E_{\mathbf{k}} \equiv (\xi_{\mathbf{k}}^2 + |\phi_{\mathbf{k}}|^2)^{1/2} , \tag{A2}$$

$$u_{\mathbf{k}}^2 \equiv \tfrac{1}{2}(1+\xi_{\mathbf{k}}/E_{\mathbf{k}}) , \tag{A3}$$

$$v_{\mathbf{k}}^2 \equiv \tfrac{1}{2}(1-\xi_{\mathbf{k}}/E_{\mathbf{k}}) , \tag{A4}$$

$$\alpha_{\mathbf{k}} \equiv \phi_{\mathbf{k}}/|\phi_{\mathbf{k}}| . \tag{A5}$$

The gap function in the BCS model is given by

$$\phi_{\mathbf{k}} = \Theta(\omega_0 - |\xi_{\mathbf{k}}|)\Delta , \tag{A6}$$

where Θ is the unit-step function, Δ is the gap parameter, and $\xi_{\mathbf{k}} \equiv k^2/2m - \mu$ is the excitation energy relative to the Fermi energy. The pairing-shell thickness ω_0 is of the order of the Debye frequency in conventional superconductors.

APPENDIX B: TEMPERATURE DEPENDENCE OF $r^0(\mathbf{p})$

If the smearing of the Fermi factor is neglected ($\mu_e \gg T$), Eq. (3.7) can be integrated analytically, yielding

$$r^0(\mathbf{p}) = \tfrac{1}{2}\{\mathrm{sgn}(x_F - x)\,\mathrm{erf}(|x_F - x|) + \mathrm{erf}(x_F + x) - \pi^{-1/2}\exp[-(x_F^2 + x^2)](e^{2x_F x} - 1)/2x\} , \tag{B1}$$

for isotropic electron and positron bands, where $x \equiv p/(2m_p T)^{1/2}$, $x_F \equiv p_F/(2m_p T)^{1/2}$. The lowest-order temperature-dependent correction can be exhibited more clearly by expanding the error functions:

$$r^0(\mathbf{p}) = (\Theta(-\xi_{\mathbf{p}}) - (m_p T/2\pi)^{1/2}\{[(p_F - p)^{-1} + p^{-1}]\exp[-(p_F - p)^2/2m_p T] + (p_F + p)^{-1}\exp[-(p_F + p)^2/2m_p T] - p^{-1}\exp[-(p_F^2 + p^2)/2m_p T]\}) . \tag{B2}$$

The leading correction to Eq. (B1) is thus of the form

$$(m_p T)^{1/2}/(p_F - p)\exp[-(p_F - p)^2/2m_p T] ,$$

which is appreciable only near the Fermi edge. Incidentally, Eq. (B2) can also be directly obtained from the relation

$$J[f,p,T] = J[f,p,0] + 4\pi^3 \nabla^2 f(p) T + O(T^2) ,$$

where

$$J[f,p,T] \equiv (2\pi/T)^{-3/2} \int d^3k\, f(k)\exp(-\beta\zeta_{\mathbf{p}-\mathbf{k}}) ,$$

and

$$J[f,p,0] = (2\pi^3) f(p) .$$

APPENDIX C: $r^1(p)$ NEAR FERMI EDGE AND AT ZERO MOMENTUM

Some analytical results can be derived for the normal state near $p = 0$ and $p = p_F$. Substituting Eq. (4.1) into Eq. (3.12), we obtain

$$r^1(0) = (4/\pi q_s)[\pi/2 - \tan^{-1}(p_F/q_s)], \quad \text{(3D)} . \tag{C1}$$

Replacing $d^3k/(2\pi)^3$ by $d^2k/(2\pi)^2$ in Eq. (3.12) and (for simplicity) setting $g(q) = 1$ in Eq. (4.4), we find the corresponding result for a two-dimensional system:

$$r^1(0) = \ln[(p_F + 2)/p_F] \quad \text{(2D)} . \tag{C2}$$

With Eqs. (C1) and (C2), we obtain in the high-density limit ($p_F \to \infty$):

$$r(0) = 1 + A/p_F , \tag{C3}$$

where (Ref. 37) $A_{3D} = 4/\pi$ and $A_{2D} = 2$. The constant A is a measure of the strength of the Coulomb correlations between the positron and the electron liquid.

The singularity in the integrand of Eq. (3.12) at $p = p_F$ dominates the behavior in the immediate vicinity of the Fermi edge. In the 3D case, we find

$$r^1(p) \sim \text{const} + [(p_F - p)/p_F]\ln[(p_F - p)/p_F] . \tag{C4}$$

A logarithmic singularity occurs in two dimensions,

$$r^1(p) \sim \text{const} + \ln[(p_F + p)/(p_F - p)] . \tag{C5}$$

The singularities in Eqs. (C4) and (C5) result from the zero in the energy denominator of Eq. (3.14) at $p = k = p_F$, and are analogous to susceptibility singularities. As in the case of Kohn anomalies, the effects increase as the dimension is reduced.

*Permanent address.

[1]See, e.g., *Positron Annihilation*, edited by P. C. Jain, R. M. Singru, and K. P. Gopinathan (World Scientific, Singapore, 1985).

[2]For a brief summary of the pre-high-T_c position, see C. K. Majumdar in Ref. 1, p. 34.

[3]Y. C. Jean, H. Nakanishi, J. Kyle, S. J. Wang, P. E. A. Turchi, R. H. Howell, A. L. Wachs, M. J. Fluss, R. L. Meng, H. P. Hor, J. Z. Huang, and C. W. Chu, in *Positron Annihilation*, edited by L. Dorikens-VanPraet, M. Dorikens, and D. Segers (World Scientific, Singapore, 1989), p. 922.

[4]D. R. Harshman, L. F. Schneemeyer, J. V. Waszczak, Y. C. Jean, M. J. Fluss, R. H. Howell, and A. L. Wachs, Phys. Rev. B **38**, 848 (1988).

[5]Y. C. Jean, J. Kyle, H. Nakanishi, P. E. A. Turchi, R. H. Howell, A. L. Wachs, M. J. Fluss, R. L. Meng, H. P. Hor, J. Z. Huang, and C. W. Chu, Phys. Rev. Lett. **60**, 1069 (1988); Y. C. Jean, H. Nakanishi, M. J. Fluss, A. L. Wachs, P. E. A. Turchi, R. H. Howell, Z. Z. Wang, R. L. Meng, H. P. Hor, Z. J. Huang, and C. W. Chu, J. Phys. C **1**, 2989 (1989).

[6]S. G. Usmar, P. Sferlazzo, K. G. Lynn, and A. R. Moodenbaugh, Phys. Rev. B **36**, 8854 (1987).

[7]S. Ishibashi, Y. Suzuki, R. Yamamoto, T. Hatano, K. Ogawa, and M. Doyama, Phys. Lett. A **128**, 387 (1988).

[8]E. C. von Stetten, S. Berko, X. S. Li, R. R. Lee, J. Brynestead, D. Singh, H. Krakauer, W. E. Pickett, and R. E. Cohen, Phys. Rev. Lett. **60**, 2198 (1988).

[9]Although several groups have observed changes in positron characteristics near T_c, the increase in the bulk lifetime below T_c reported in Refs. 3–5 has not yet been confirmed by other workers.

[10]K. O. Jensen, R. M. Nieminen, and M. J. Puska, in *Positron Annihilation,* Ref. 3, p. 892; J. Phys. C **1**, 3727 (1989).

[11]S. G. Usmar, K. G. Lynn, A. R. Moodenbaugh, M. Suenaga, and R. L. Sabatini, Phys. Rev. B **38**, 5126 (1988).

[12]The existence of such a shift could be investigated using the density-functional theory for superconductors developed by L. N. Oliviera, W. Kohn, and E. K. U. Gross, Phys. Rev. Lett. **60**, 2430 (1989).

[13]B. Chakraborty, Phys. Rev. B **39**, 215 (1989).

[14]T. McMullen, Phys. Rev. B (to be published).

[15]D. N. Tripathy and M. Bhuyan, in *Positron Annihilation,* Ref. 1, p. 91.

[16]A preliminary report on this work appeared in R. Benedek and H.-B. Schüttler, Bull. Am. Phys. Soc. **33**, 345 (1988).

[17]J. P. Carbotte and S. Kahana, Phys. Rev. **139**, A213 (1965).

[18]S. Berko, in *Positron Solid State Physics,* edited by W. Brandt and A. Dupasquier (North-Holland, New York, 1983); R. N. West, in *Positron Annihilation,* in Ref. 1.

[19]C. K. Majumdar, Phys. Rev. A **140**, 227 (1965).

[20]In the zero-temperature theory (Ref. 17), the brackets denote a ground-state expectation values for a system with a single positron.

[21]J. R. Schrieffer, *Theory of Superconductivity* (Benjamin, New York, 1964).

[22]G. D. Mahan, *Many Particle Physics* (Plenum, New York, 1981), p. 825.

[23]R. E. Prange, Phys. Rev. **129**, 2495 (1963).

[24]F. Stern, Phys. Rev. Lett. **18**, 546 (1967); see also A. Isihara, in *Solid State Physics,* edited by H. Ehrenreich and D. Turnbull (Academic, New York, 1989), Vol. 42, p. 271.

[25]By an analysis similar to that of McMullen (Ref. 14), one obtains for a two-dimensional system $f(x)=(1+x^2)^{-1/2}-1$.

[26]K. E. Gray, Mod. Phys. Lett. **B2**, 1125 (1988); R. T. Collins, Z. Schlesinger, F. Holtzberg, and C. Feild, Phys. Rev. Lett. **63**, 422 (1989).

[27]A. Bansil, R. Pankaluoto, R. S. Rao, P. Mijnarends, W. Dlugosz, R. Prasad, and L. C. Smedskjaer, Phys. Rev. Lett. **61**, 2480 (1988).

[28]D. Singh, W. E. Pickett, R. E Cohen, H Krakauer, and S. Berko, Phys. Rev. B **39**, 9667 (1989).

[29]H. Sormann, *Positron Annihilation,* in Ref. 3, p. 272.

[30]B. Muhlschlegel, Z. Phys. **155**, 313 (1959).

[31]The moments M_j in the normal and superconducting states are nearly identical if $r(p)$ for the normal state is constant from p_- to p_F.

[32]S. Kahana, Phys. Rev. **129**, 1622 (1963).

[33]E. Boronski, Z. Szotek, and H. Stachowiak, Phys. Rev. B **23**, 1785 (1981).

[34]D. N. Lowy, Phys. Rev. B **26**, 60 (1982).

[35]J. Arponen and E. Pajanne, J. Phys. F **9**, 2359 (1979).

[36]L. C. Smedskjaer, B. W. Veal, D. G. Legnini, A. P. Paulikas, and L. J. Nowicki, Phys. Rev. B **37**, 2330 (1988).

[37]The relation for A_{3D} is consistent with numerical results given by E. Bonderup, J. U. Anderson, and D. N. Lowy, Phys. Rev. B **20**, 883 (1979).

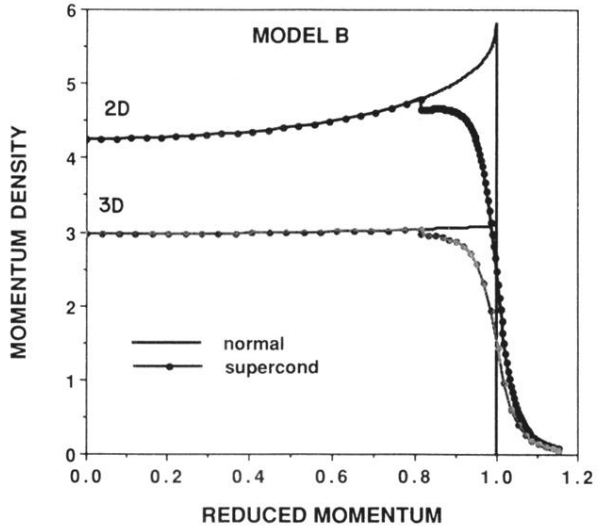

FIG. 1. Momentum density $r(p)=r^0(p)+r^1(p)$ vs reduced momentum p/p_F calculated for model B (cf. Table I). The curves with discontinuities at $p/p_F=1$ correspond to the normal state and the dotted curves represent the superconductor. The small discontinuities that occur in the superconducting case at $p_-=0.815$ and $p_+=1.16$ result from the abrupt cutoff of the gap function at ω_0, as given in Eq. (A6). A momentum density of unity would correspond to a noninteracting system.